JOURNAL OF AIRCRAFT
Vol. 32, No. 5, September–October 1995

Rotor Aerodynamic Loads Computation Using a Constant Vorticity Contour Free Wake Model

Todd R. Quackenbush,* Daniel A. Wachspress,† and Alexander H. Boschitsch‡
Continuum Dynamics, Inc., Princeton, New Jersey 08543

The prediction of vibratory loads on helicopter rotors depends critically on closely coupled interactions between wake-induced aerodynamic loading and structural deformation. Previous rotary wing aerodynamic analyses have typically used models lacking important features of the actual wake structure. This article summarizes the development of a comprehensive analysis of isolated rotors that employs a significantly improved approach to wake simulation. The model discretizes the sheet of vorticity that trails from each blade by laying out vortex filaments along contours of constant sheet strength. In this constant vorticity contour (CVC) wake model, the filaments are composed of curved vortex elements that distort freely in response to the local velocity field. This approach captures the wake of the full span of each rotor blade and includes many features of the complex vorticity field absent from earlier, more simplified models. This article outlines the capabilities of a rotor analysis that incorporates the CVC approach to wake modeling and presents results concentrating on configurations where wake/blade interaction is of particular importance for modeling unsteady airloads.

Nomenclature

c	=	blade chord
dT/dr	=	thrust force distribution along the span (shaft axis)
i_r, i_ψ	=	unit vectors parallel and perpendicular to the blade span, respectively
q	=	flowfield velocity vector
R	=	rotor radius
r	=	radial distance from rotor hub
r_c	=	vortex core radius
v_θ	=	vortex swirl velocity
Γ	=	bound circulation on the blade
γ	=	vector vorticity field in the rotor wake
ρ	=	air density
ρ_v	=	radial distance from vortex center
ψ	=	azimuth angle of rotor blade (zero for the blade pointing downstream)
Ω	=	rotor rotation frequency

I. Introduction

EFFORTS to predict unsteady airloads on helicopter rotors have been underway for over 30 years.[1-9] One motivation for this research has been the high level of vibration experienced by rotorcraft in a variety of flight conditions. The study of the dynamic response of rotor blades to aerodynamic loading is, in general, well advanced, whereas the prediction of the wake-induced velocities that produce this loading is more uncertain. The prediction of the velocity field induced by the rotor wake and the resulting aerodynamic loads are the primary topics of interest in this article.

The particular focus of the present work has been the development of an analysis of rotor aerodynamic loading in forward flight using an advanced model of the vortex wake. The constant vorticity contour (CVC) wake described here features a unique discretization of the wake into filamentary vortices representing constant-strength contours of vorticity in the vortex sheets that trail from each blade. The CVC model is noteworthy in that it eliminates the artificial distinction between vorticity generated by azimuthal and spanwise changes in the bound circulation on the blade (i.e., between what is conventionally termed "shed" and "trailed" vorticity), and that it provides a visually meaningful representation of the wake. Previous exploratory work[10-12] indicated the potential of this approach for obtaining improved predictions of wake-induced vibratory airloads. This article summarizes selected results from the recent development and validation of a comprehensive analysis of rotor aerodynamics in forward flight that incorporates the CVC model in the computation of the force-free wake geometry. A particular focus of this article is to demonstrate the importance of proper modeling of the structure of the vorticity field in addition to capturing the distortion of the vortex wake.

The computation of aerodynamic loads in the presence of the wake-induced flowfield is carried out in the present analysis using a vortex lattice model of the blade.[13] This model is appropriate for these calculations since it provides a more refined treatment of tip effects and vortex/blade interaction than the lifting line models used in the previous investigations.[2-5] The present analysis also employs local corrections that allow it to capture subcritical compressibility effects.[13] Although more advanced treatments of rotor blades in compressible flow have been the subject of several recent papers,[14-17] these models typically have used simplified wake models or numerical schemes that cannot presently capture detailed wake effects.

Computation of the structural response to a given blade loading has been extensively studied, and it was not the intention of the present effort to break new ground in this area. Thus, the dynamic model developed here features the implementation of a finite element analysis of blade structure drawn largely from the existing literature, as will be briefly discussed later. The complete analysis formed by the integration of this structural model with the CVC wake model and the vortex lattice load analysis has been dubbed RotorCRAFT (computation of rotor aerodynamics in forward flight). Numerous correlation studies have been carried out to assess the performance of this model in predicting unsteady aerodynamic loading on representative helicopter blades over a wide range of operating conditions.[13,18-21] Results presented here focus on moderate-to-high speed forward-flight configurations that

Received Nov. 6, 1992; revision received Dec. 21, 1994; accepted for publication April 26, 1995.

*Senior Associate. Senior Member AIAA.
†Associate.
‡Associate. Member AIAA.

exhibit blade/wake interactions for which proper modeling of the vorticity field is crucial.

II. Background

Miller[1] discussed many of the sources and consequences of vibratory airloads in helicopters, pointing out the importance of capturing wake distortion so as to properly account for unsteady loading in both low- and high-speed flight. Scully[2] developed a free-wake analysis of the rotor using two free filaments (a rolled-up tip vortex and a large-core inboard filament) to model the rotor wake. This distorted wake model succeeded in predicting certain features of the unsteady loading on rotors, though uncertainties about the modeling of close blade/wake interactions precluded accurate prediction of higher harmonic loads. Other broadly similar wake models have been developed in recent years.[3-5]

The seminal paper of Hooper[6] pointed out the inadequacy of these types of models in predicting the nearly impulsive airloading events that occur in a broad range of rotor designs. Hooper's particular focus was on cases in high-speed cruise where it was found that higher harmonic loading was dominated by a relatively discrete event near the blade tip on the advancing side (Fig. 1). During such interactions the blade experiences a sharp upward and then downward loading. This up–down pulse, which is clearly an important contributor to the overall higher harmonic airloading, appeared to be due primarily to aerodynamic interaction with the wakes produced by previous blades. Hooper documented the inability of conventional rotor wake models to compute the behavior observed in the experimental data, a result suggesting that some aspects of the traditional approach to rotor wake aerodynamics must be inadequate. Such models have typically treated the wake using a single-tip vortex of varying strength trailed from the blade tip. Recent work by Miller[7] and Johnson[8] has been directed in part toward repairing some of the shortcomings in previous single-tip vortex models, as the free wake model described by Egolf[9] has been.

Any wake model designed to capture the important features of the loading experienced by rotor blades must include an adequate treatment of wake-induced forcing. Figure 2 illustrates the rapid, complicated load variations typical of those that commonly occur on the advancing side of rotors in forward flight. Around $\psi = 90$ deg there can exist a region of negative load at the tip along with a relatively gradual spanwise load variation inboard, with the maximum load shifted far away from its typical location near the tip. These load variations generate a complex wake through which the following blades pass. Models that oversimplify the wake structure will, in general, fail to accurately predict unsteady airloads in forward flight, even if an advanced treatment of the transonic flow near the tip is invoked.

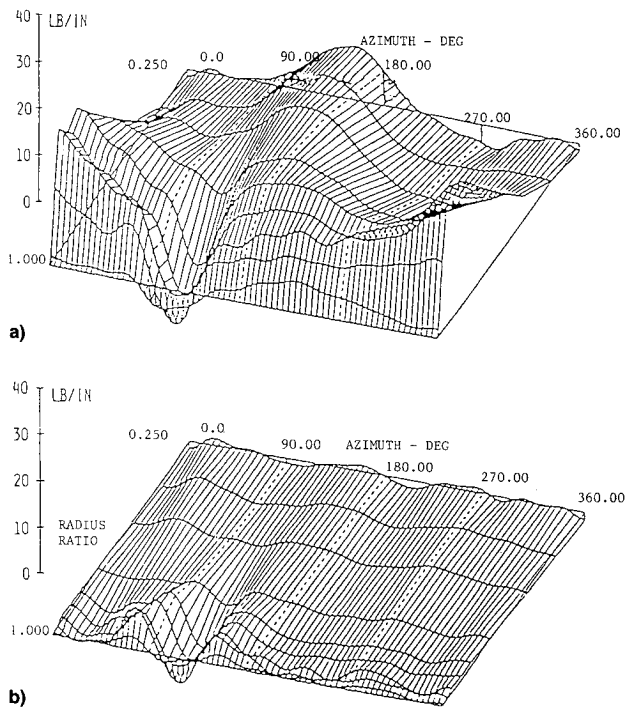

Fig. 1 Linear surface plots of aerodynamic load distribution of the H-34 main rotor at advance ratio 0.39 (from Ref. 6). Harmonics a) 0–10 and b) 3–10.

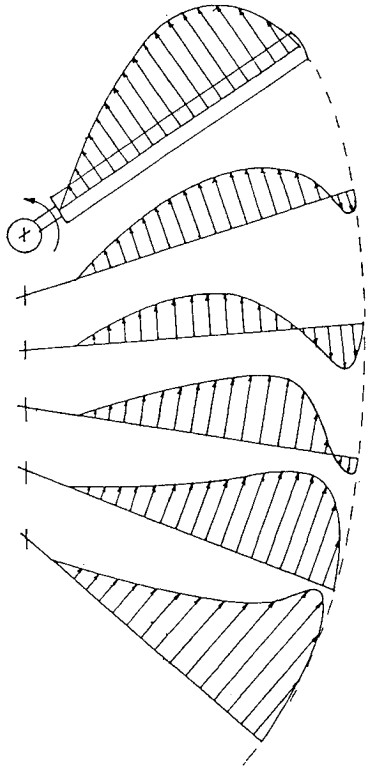

Fig. 2 Typical load variations on the advancing side in high-speed flight.

The original work on the CVC model was initiated by Bliss[10] and was directed at demonstrating the applicability of this model for the prediction of rotor airloads in high-speed flight. The CVC wake analysis was designed to accommodate a very general description of the wake associated with realistic blade loads. The wake structure accounts for the effects of spatial and temporal load variations on the generating blade. Preliminary development of these concepts[10-12] produced promising initial results toward the prediction of the vibratory airloading of rotors. However, despite its importance in predicting helicopter vibration, hf airloading cannot be considered in isolation. The complete aerodynamic load calculation on the rotor, including the coupling to performance, trim, and blade dynamics calculations, must be considered. For this reason, considerable effort was required to supplement previous exploratory work to construct a comprehensive analysis of rotor aerodynamics. Results presented in this article concentrate on wake structure; additional discussion of relevant analysis development is given in Refs. 13, 19, and 21.

III. CVC Full-Span Free-Wake Modeling

The purpose of a free-wake analysis is to simulate in detail the actual shape and motion of the wake trailed from each rotor blade. The wake is represented by vortex filaments trailed from the blade. Each trailing filament is composed of a string of individual vortex elements connected at collocation points. The velocity field of these individual vortex elements is de-

termined through numerical evaluation of analytical expressions based on the Biot – Savart law. The overall wake velocity field is evaluated numerically by summing the contributions of the individual elements. Traditionally, straight-line elements have been used for this purpose.[2-5] An alternate approach was developed using a more sophisticated curved element.[22,23] Curved elements have also been applied to work on the wakes of hovering rotors as well as simulations in low- and moderate-speed forward flight.[23-25] The documented success of curved elements in wake modeling is an important facet of the forward flight wake model described in this article.

To illustrate the method by which the CVC wake is generated, consider the idealized sequence of advancing side load distributions sketched in Fig. 2. Spanwise variations in the blade load are responsible for the trailed component of wake vorticity and temporal (i.e., azimuthal) variations are responsible for the shed component. Given a bound circulation distribution along the span, $\Gamma(r, \psi)$, the wake that trails from the blade consists of a continuous sheet of vorticity whose strength as it leaves the blade is $\gamma(r, \psi)$. This can be represented by

$$\boldsymbol{\gamma} = \gamma_r \boldsymbol{i}_r + \gamma_\psi \boldsymbol{i}_\psi \tag{1}$$

where $\boldsymbol{i}_r$ and $\boldsymbol{i}_\psi$ are defined parallel to the span and the chord of the blade, respectively, at the time of release of the wake. The components of vorticity are given by

$$\gamma_r = \frac{1}{\Omega r} \frac{-\partial \Gamma(r, \psi)}{\partial t} \tag{2}$$

$$\gamma_\psi = \frac{-\partial \Gamma(r, \psi)}{\partial r} \tag{3}$$

whereas the magnitude of the vorticity is

$$\gamma = |\boldsymbol{\gamma}| = \sqrt{\gamma_r^2 + \gamma_\psi^2} \tag{4}$$

Note that the strength of the wake sheet may be zero and that each component may reverse sign, depending on the strength and rate of change (spatial or temporal) of the bound circulation.

Figure 3 shows an idealized wake vorticity field corresponding to the load variations in Fig. 2. The wake here is shown in terms of a finite number of contours of constant sheet strength, i.e., lines of constant γ are depicted (ignoring any vertical distortion). Because increments in γ are constant between each contour line, the amount of circulation contained between any two contour lines on the sheet is constant. This increment in circulation is related to the bound circulation on the blade as follows:

$$\Delta\Gamma = \int_r^{r+\Delta r} -\gamma(r, \psi)\, dr = \Gamma(r + \Delta r, \psi) - \Gamma(r, \psi) \tag{5}$$

If the origination points of contour lines (denoted "release points") are spaced radially along the blade corresponding to fixed increments in bound circulation, then the radial distance between the contour lines will be a direct measure of the gradient in bound circulation along the blade. That is, if $\Delta\Gamma$ is held constant, the approximate relationship

$$\frac{\partial \Gamma(r, \psi)}{\partial r} \cong \frac{\Delta\Gamma}{\Delta r(r, \psi)} \tag{6}$$

indicates that the contour spacing will be inversely proportional to the spanwise circulation gradient. Thus, contour lines will be tightly spaced in the radial direction where gradients of bound circulation are high, as is typically true near the blade tip at most azimuth angles. As Fig. 2 makes clear, however, realistic blade load variations do not always produce large bound circulation gradients near the blade tips. Gradients are often shallow at the advancing tip in high-speed flight, and so the wake may take on a more sheet-like character, rather than rolling up into a concentrated tip vortex. Conversely, bound circulation gradients may not always be shallow in certain regions. Note in particular that the radial gradients near the blade root in forward flight may be relatively large compared to the weak gradients typically seen in the inboard loading distribution of hovering rotors. Thus, unlike the diffuse inboard wakes usually present on rotors in hover, concentrated vortical structures may be present trailing from the inboard region of rotors in high-speed flight.

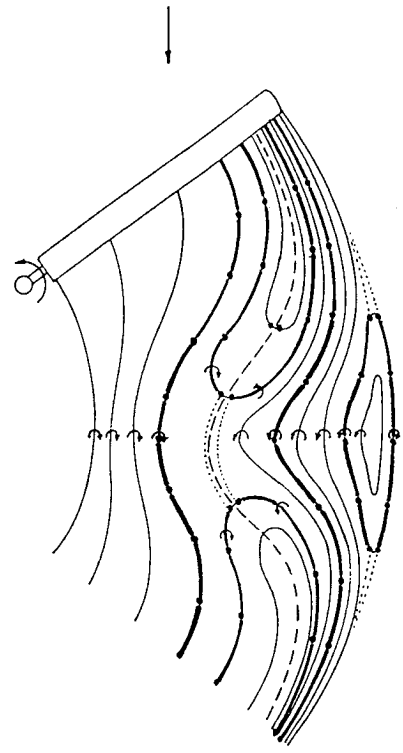

Fig. 3 Contours of constant sheet strength in the wake on the advancing side modeled with curved vortex elements.

Note also that the tangent to the contour line at any point determines the direction of the local vorticity vector $\boldsymbol{\gamma}$ with the trailed and shed vorticity simply being components of the resultant vector $\boldsymbol{\gamma}$. While conceptually convenient to retain this terminology in some cases, it is desirable to employ a wake discretization like the CVC model that removes the artificial distinction between these two quantities and treats the vector vorticity field in a unified manner. In principle, one could discretize the wake into continuous sheet elements, but this has proved awkward in the past[2]; curved sheet elements that smoothly capture the distortion of the wake sheet are computationally expensive, while a model using simpler flat sheet elements tends to develop kinks and gaps. It was judged preferable to develop a wake model that exploits the accuracy and efficiency of curved elements and builds on the insights gained from examining the contours of constant wake vorticity. The present model represents the wake by laying down curved vortex elements along the contours of constant wake strength (Fig. 3). To conserve circulation in the wake, these filaments are assumed to contain all of the vorticity trailed between adjacent release points. This means that all of the filaments will have equal and constant strength $\Delta\Gamma$ along their length.

The shed and trailed vorticity is thus accounted for by the fact that the direction of the tangent vector to the resultant elements changes continuously even though the strength of each filament is constant. Using the CVC approach, on the

average only half as many elements are required as in the straight-line lattice wake method, where the local vorticity vector is represented by two discrete straight elements.[9] Thus, the use of curved elements means that fewer, relatively large elements can be used to accurately represent the vector vorticity field in the wake. This gives the full-span CVC wake model a substantial advantage in efficiency relative to a full-span model using a lattice of straight elements. This advantage is in addition to the fact that the filament locations represent contours of vorticity that allow the structure and strength of the wake to be perceived visually. Once the wake is generated, its spatial evolution proceeds in the same way as previous Lagrangian models. The key difference is that the wake trails from the full span of the blade and is not a simple root/tip filament pair. This full-span approach allows for the automatic appearance, evolution, and disappearance of the wake of opposite-sign circulation zones near the tip as they occur.

IV. Overview of the Wake Model and Blade Aerodynamic Model

The analysis begins with an estimate of the spanwise-bound circulation distribution at a set of azimuthal locations computed using a vortex lattice treatment of the blade loading in conjunction with a simple uniform inflow model. The spanwise release points for the individual filaments are found by interpolation between the fixed calculation points along the span. The release points are updated as the circulation distribution changes during the calculation. Not only do release points shift along the blade span, but some also disappear and reappear as the maximum circulation decreases and increases. This disappearance and reappearance corresponds to the formation of loops in the wake.

Although the use of the full-span CVC wake model is important to the computation of wake motion and wake-induced velocities in the region near the rotor, it is in general computationally expensive to retain this model over the full length of a semi-infinite wake. Thus, provision has been made for collapsing the full-span CVC wake into a freely distorting root/tip vortex pair for regions suitably far downstream of the rotor disk. For regions still further downstream, the freely distorting trailers are replaced by a prescribed filament pair that captures the effect of the full semi-infinite wake through a combined analytical/computational model; the hierarchy of wake models is described in more detail in Ref. 13.

As with all Lagrangian wake models using vortex filaments, a vortex core is required to remove singularities from the flowfield. Previous investigations[2,3,8,9] found that load calculations are sensitive to the particular core size chosen. One of the objectives in formulating the current model was to remove as much of this sensitivity as possible. First, it should be noted that the full-span CVC wake model itself contributes substantially to the aim of weakening the modeling role of the core. Alternative models, such as using single free tip filaments, must of necessity use adjustments in the core size to produce changes in the wake-induced flowfield that are attributable to changes in wake structure brought about by variations in spanwise and azimuthal loading. Since such effects are automatically captured with the full-span CVC wake analysis, one possible ambiguity has been removed.

However, since filamentary vortices are still used, some effective core structure must be imposed to remove the flowfield singularities associated with curved vortices. The core model used here is the one originally proposed by Scully[2]; the swirl velocity profile is

$$v_\theta = \frac{\Gamma}{2\pi} \frac{\rho_v}{\rho_v^2 + r_c^2} \tag{7}$$

This core model retains half of the vorticity associated with the vortex inside r_c and leaves half outside. The issue of the selection of the core radius itself remains. Currently, the core radii vary from filament-to-filament and along filaments from azimuth-to-azimuth. In keeping with the spirit of the discretization of the wake, which places curved filaments on contour lines of constant strength of the wake sheet trailing from each blade, the local core radius is based on the distance between vortex release points at each azimuth. The core radius becomes the average distance to the neighboring release points on either side (at a given azimuth) with special cases at the root, tip, and center of each zone. Thus, the default core radius is chosen so as to have the flowfield generated by adjacent trailed vortices resemble that of a vortex sheet. In the current analysis, bounds can be placed on the core size and, if desired, particular core radii can be chosen for each filament. However, in the correlation runs discussed later, the core radius assigned to each filament was determined as just described, with no alterations for individual cases. It is judged that this approach is consistent with the overall aim of removing as much arbitrariness as possible from the analysis of rotor airloads.

For modern rotor blades with complex planforms, it is advantageous to use a vortex lattice to analyze aerodynamic loading. The particular model employed here focuses primarily on thin lifting surfaces with no side- or leading-edge separation.[26,27] The rotor blade is represented by a surface consisting of vortex quadrilaterals. Four constant strength straight-line vortices form the sides of each quadrilateral except at the trailing edge of the blade where a modified vortex quadrilateral without the downstream line vortex is used. Control points are located at the center of each quadrilateral. This formulation allows substantial flexibility in the specification of the blade planform; the lattice can be divided into an arbitrary number of spanwise segments, with separate linear distributions of twist, taper, and sweep within each. The spacing of the quadrilaterals in a vortex lattice analysis is an important consideration.[28] The judicious selection of the density, spacing, and orientation of the quadrilaterals can considerably enhance the efficiency and rate of convergence of the blade loading. All the calculations discussed in this article feature uniform spacing of vortex quadrilaterals both in the chordwise and spanwise directions.

The solution method used to find the bound circulation given this lattice is essentially a straightforward implementation of the classical approach described in the literature on lattice methods for fixed wing applications (e.g., Ref. 27). The normal velocity induced by each blade quadrilateral at each control point is determined for unit circulation strength to yield an array of influence coefficients. The normal velocity component at each control point due to the wake induced velocity, freestream, and blade motion is also determined. A matrix equation is then solved to determine the bound circulation on the blade quadrilaterals that satisfies flow tangency at the control points. These bound circulation values are subsequently used to calculate the forces and moments on each segment of the blade through application of the Joukowski law.

The forces predicted by the basic vortex lattice analysis must be modified to include predictions of profile (viscous and pressure) drag for performance calculations, as well as the effect of compressibility on the sectional lift and moment. Other modifications are necessary to account for stall, yawed flow, and as well as to smooth the flowfield induced by the extreme near wake.[13] To introduce forces generated by profile drag into the calculation, the only practical approach at present is the use of two-dimensional airfoil data. This coupling uses tabulated values for sectional lift and sectional drag coefficients as a function of both Mach number and sectional angle of attack. The computed lift coefficient of a section is used in the look-up process; the effective angle of attack serves only as an intermediate variable.

Compressibility has an important effect on performance for Mach numbers typical of modern rotors. Some of this effect

is obtained through the Mach number dependence in the two-dimensional airfoil data used for profile drag coefficients. However, compressibility also has a significant impact on the lift generated by airfoils at specified angles of attack, and so its influence on thrust and induced power must be considered as well. For two-dimensional thin airfoils, treatments like the Prandtl – Glauert correction to lift curve slope are useful for including compressibility effects. In vortex lattice calculations, transformations that are similar in spirit, but more elaborate in detail, must be invoked. Currently, a transformation of the blade geometry is used that involves stretching the chord of the blade at a given radial station based on the local Mach number at that section.[25] It should be noted that a desirable objective of future work on rotor load predictions using the CVC wake model would be the incorporation of a transonic flow solver. Boschitsch and Quackenbush,[14] building in part on previous investigations,[15–18] have laid the groundwork for the application of a more general three-dimensional Euler analysis for rotor aeroelastic calculations in transonic flow.

V. Formulation of the Rotor Blade Dynamic Model

The structural deformation of the helicopter blade is important to the evaluation of the performance and unsteady loading of a helicopter in forward flight. Thus, a realistic finite element representation of the blade has been incorporated in the present analysis. This section outlines the formulation of the dynamic model and briefly discusses its capabilities and limitations. Further discussion can be found in Refs. 18–21.

The particular finite element model used here to represent the helicopter blade accounts for extension, twist, and transverse bending displacements. To accurately simulate these deformations, the blade is discretized into a number of beam finite elements each having a total of 14 degrees of freedom (DOF). Stiffness properties for each element are computed from the cross-sectional geometry and material properties supplied by the user. Similarly, the blade mass distribution is used to both define elemental mass matrices and also to compute the contributions of blade rotation inertia forces to the stiffness matrices (geometric stiffening) and nodal forces. The resulting elemental mass and stiffness matrices are then assembled and any constrained DOF eliminated to finally yield the corresponding global matrices for the complete blade structure. The approach taken is similar to previous implementations of finite element methods for rotorcraft applications[29] and applied to static deflection.[30] The blade model assumes the blade displacements are sufficiently small, that linear constitutive relations between stress and strain are applicable and that the twist, bending, and extension defor-

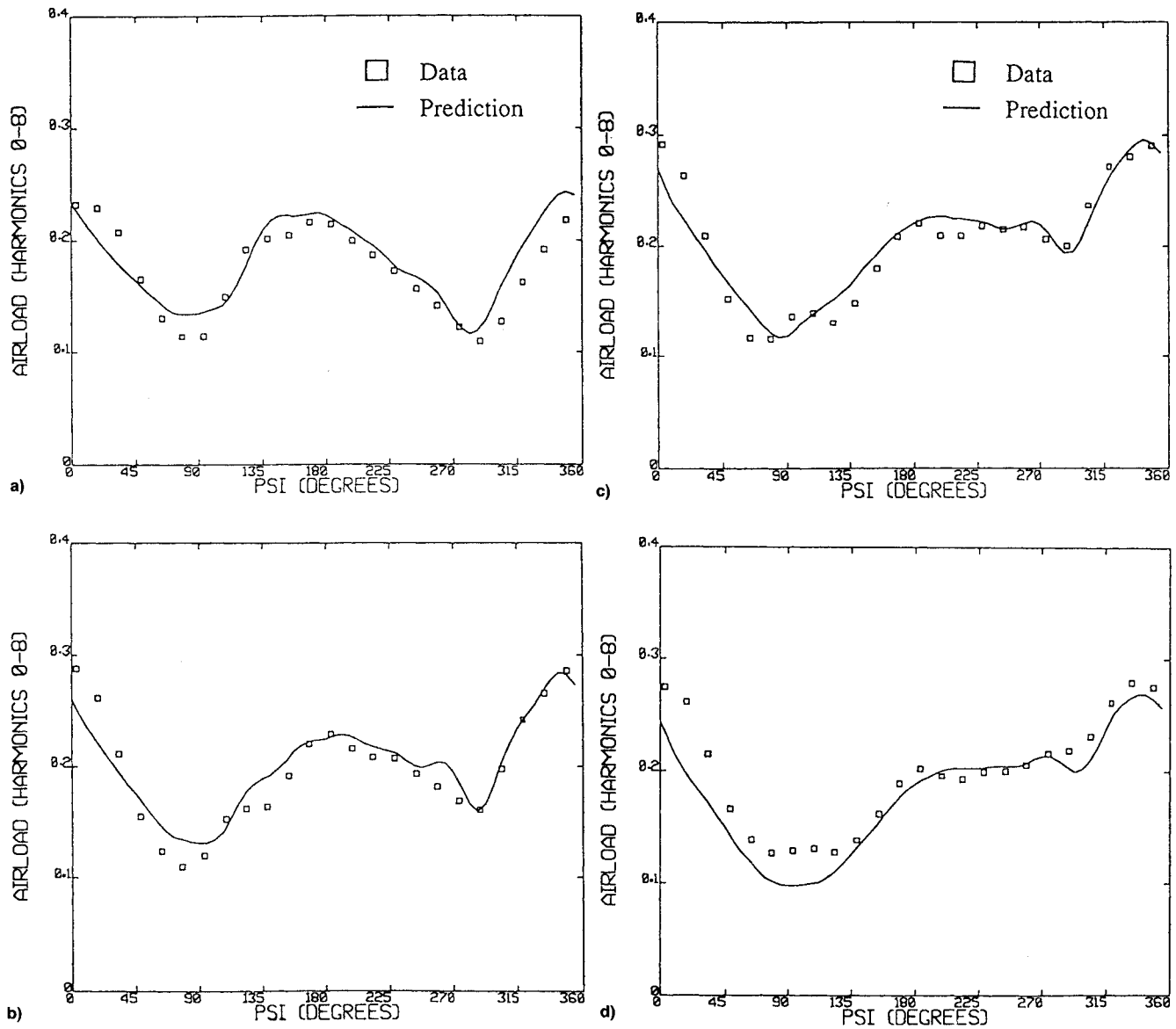

Fig. 4 H-34 flight test plot of nondimensional airload vs azimuth, advance ratio 0.29. r/R = a) 0.75, b) 0.85, c) 0.9, and d) 0.95.

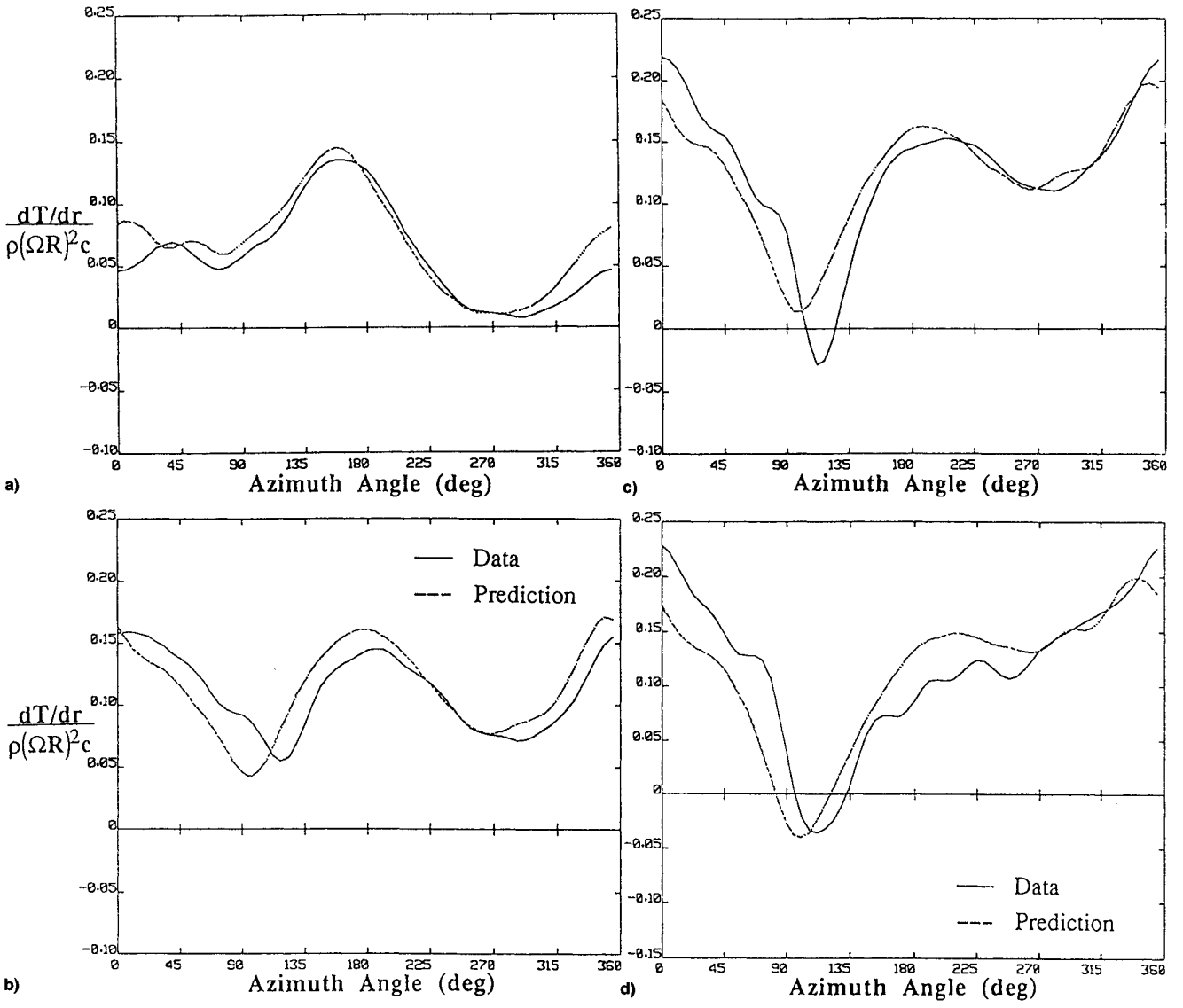

Fig. 5 Nondimensional sectional thrust vs azimuth angle for the H-34 rotor: advance ratio 0.39, −5-deg shaft angle. r/R = a) 0.55, b) 0.85, c) 0.75, and d) 0.95.

mations may be linearly superimposed. Also, the blade material is assumed to be isotropic, the stress – strain relation to obey Hooke's law, and the elastic axis to be continuous along the blade.

The resulting mass and stiffness matrices serve as inputs to a standard eigenvalue problem that must be solved to obtain the modal frequencies and shapes for the finite element model. The mode shapes are used to compute generalized modal forces from the distributed aerodynamic forces; these modal forces drive the corresponding modal responses. These responses in turn are used in conjunction with the mode shapes to determine the instantaneous displacements and velocities at any point along the blade. Finally, the blade deformations and deformation rates provide the necessary information to update the flowfield and aerodynamic forces. The particular modes retained in the dynamic analysis can be specified by the user to facilitate comparisons of the importance of individual deflection modes.

VI. Data Correlation Studies

The present analysis has correlated reasonably well with data for a wide variety of rotor configurations.[13,18–21] The results presented in this article focus on correlation with the high-speed H-34 test data that was identified by Hooper[6] as an area where current rotor/wake models have difficulty predicting aerodynamic loads. The nearly impulsive blade/wake interactions characteristic of these flight conditions are well suited for evaluating the effectiveness of the CVC full-span wake model.

References 31 – 33 contain data on unsteady aerodynamic loading from a variety of flight tests and wind-tunnel tests. Seven of these cases representing both low- and high-speed flight are analyzed in Ref. 13; of these seven, four cases involving high-speed flight are considered here. The first case is drawn from Ref. 32, and deals with an H-34 helicopter at an advance ratio of 0.29 and at a shaft angle of attack of −6.9 deg. The rotor radius was 28 ft with a blade chord of 1.36 ft, a NACA 0012 airfoil section, and −8 deg of linear twist. The tip speed for this case was 690 fps, whereas the thrust coefficient was 0.0056. In each of the calculations, the rotor was trimmed to zero first harmonic flapping to simulate the zero hub moment condition of an aircraft in free flight.

The computations were carried out using a 30 × 1 (i.e., 30 spanwise and 1 chordwise) grid of vortex quadrilaterals on the blade and a four-mode dynamic model, consisting of rigid flapping, the first two elastic bending modes of the blade, and the first elastic torsion mode. The calculation used 24 time steps per revolution and two turns of free wake, with 16 CVC wake filaments trailing from the blade span. Three rotor revolutions of simulated time sufficed to converge the calculation because of the convection dominance of the freestream. De-

fault core sizes were used for this case as well as for subsequent H-34 calculations. The thrust loading dT/dr (or "airload") was computed at several radial stations. The results for the advance ratio 0.29 case are shown in Fig. 4 for $r/R = 0.75$, 0.85, 0.9, and 0.95, and exhibit consistently good correlation with the measured loads.

Hooper[6] discussed the measured airloads from Ref. 31. The data clearly exhibits some of the dominant mechanisms that lead to large vibratory airloads in high-speed forward flight (Fig. 1). The principal physical characteristics of the H-34 blade were the same as discussed previously, though the rotor's angular velocity for this test was 23.2 rad/s, yielding a rotor tip speed of 650 fps, or roughly Mach 0.58 at standard sea-level conditions. Calculations for this case were undertaken using a blade dynamic model that included three out-of-plane bending modes (rigid flap mode and two elastic bending modes) as well as the first elastic torsion mode. In each case, the computations were trimmed to the measured thrust coefficients and first harmonic flapping amplitudes given in the experimental results; in all cases, the nominal thrust coefficient was 0.0037. Here, a vortex lattice grid using three quadrilaterals chordwise and 30 spanwise was used.

The computations discussed in Ref. 13 focus on three cases at an advance ratio 0.39 and at shaft angles of attack -5, 0, and $+5$ deg. These cases are of particular interest because they involve close interaction of the rotor wake with following blades, thus the modeling of the rotor wake plays an important role.

Figure 5 shows the measured and predicted time histories of the nondimensional thrust loading at four radial stations for the -5-deg case. The airload at $r/R = 0.55$ is well predicted. A phase error appears at $r/R = 0.75$ and both the size and phasing of the major event in the second quadrant are not well predicted at $r/R = 0.85$. However, both features improve for stations nearer the tip, where the size of the pulse in the vicinity of $\psi = 90$ deg is closer to the data and the phasing of the loading also becomes considerably closer. Figure 6 shows a similar pattern for the loading in the case of 0-deg shaft angle; close correlation inboard and near the tip and more significant errors in level and phasing for intermediate stations. Figure 7 shows slightly better results for the shaft angle $+5$-deg case. The loading inboard and outboard for this case is again well predicted, but here the results at $r/R = 0.85$ are noticeably improved, both in phase and magnitude over the -5- and 0-deg cases.

Despite the deviation in phase and magnitude at $r/R = 0.75$ and $r/R = 0.85$, these results indicate that many of the features of the airloading are being modeled correctly for the H-34 case. A topic of special interest at this point is the source of the aerodynamic loading that contributes to vibratory loads

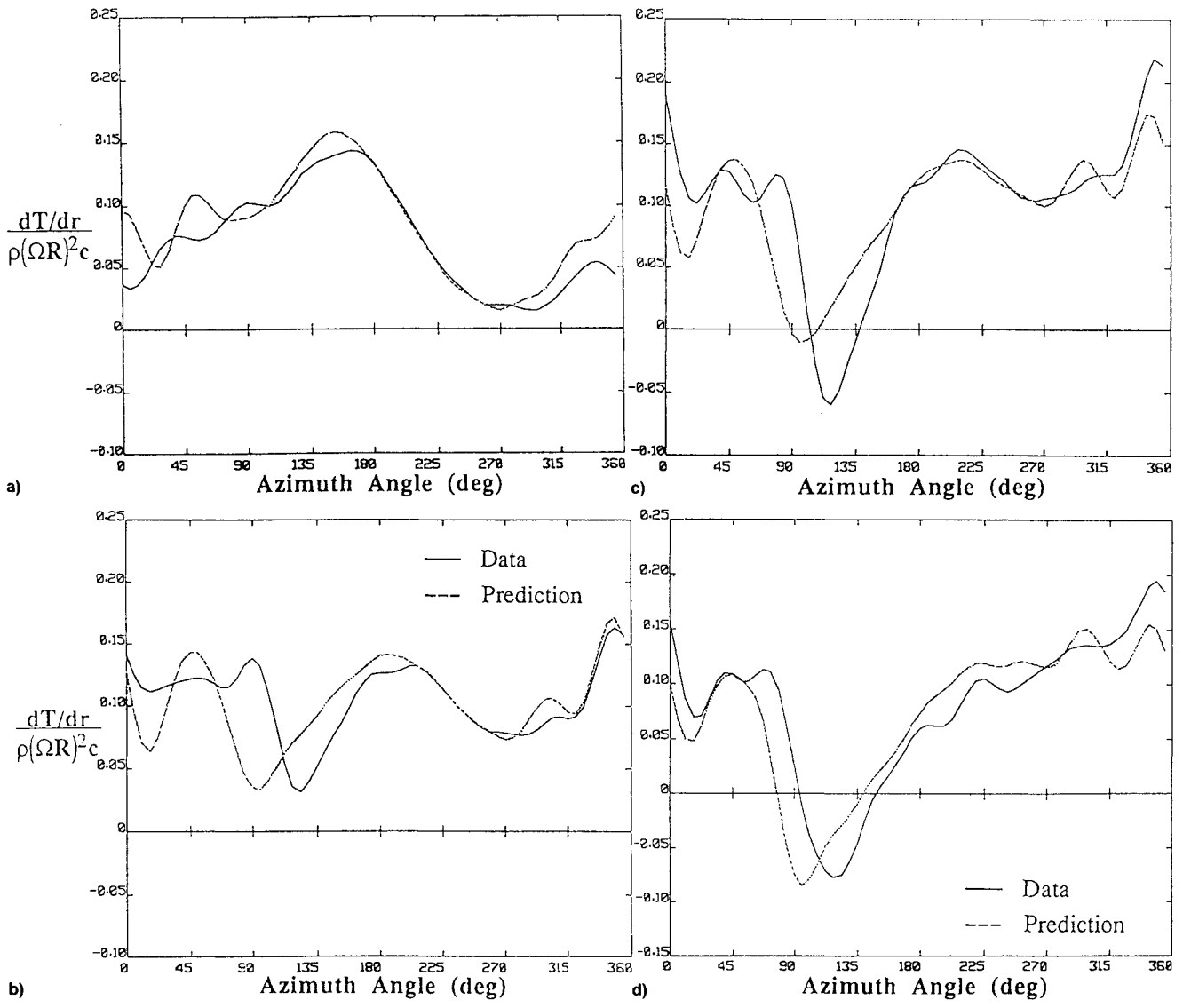

Fig. 6 Nondimensional sectional thrust vs azimuth angle for the H-34 rotor: advance ratio 0.39, 0-deg shaft angle. r/R = a) 0.55, b) 0.75, c) 0.85, and d) 0.95.

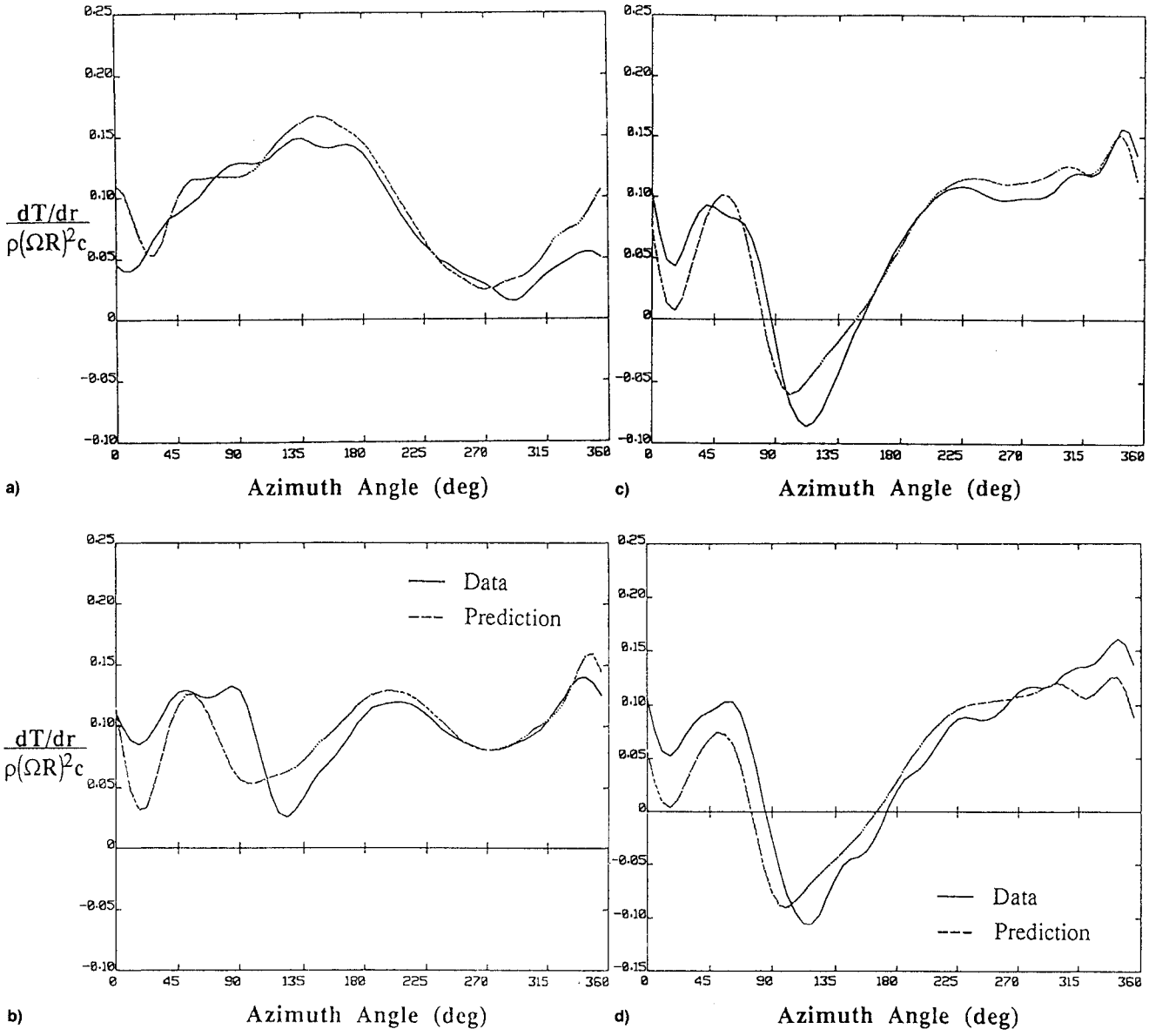

Fig. 7 Nondimensional sectional thrust vs azimuth angle for the H-34 rotor: advance ratio 0.39, +5-deg shaft angle. r/R = a) 0.55, b) 0.75, c) 0.85, and d) 0.95.

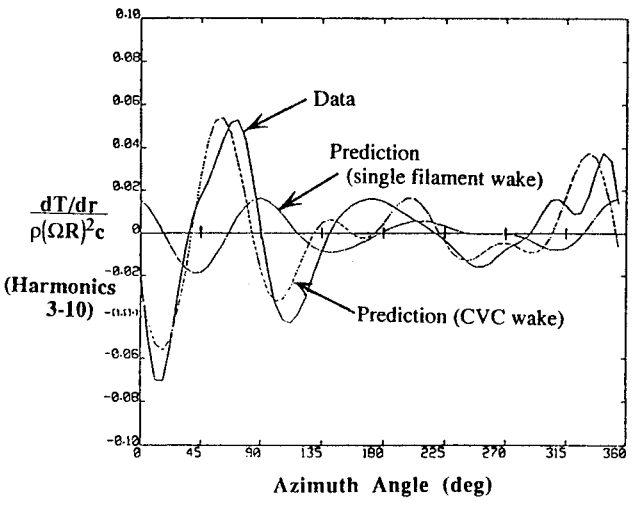

Fig. 8 Comparison of predicted and measured vibratory airloads for the H-34 at advance ratio 0.39, shaft angle +5 deg, r/R = 0.9; single filament wake and full CVC wake.

on the rotor. For this study, attention was focused on the ability of the full-span CVC wake to model the components of the rotor loading that contribute to vibration. The H-34 is a four-bladed rotor, and so the components of the aerodynamic loading at $3P$ (three-per-revolution) and above will be the primary contributors to vibratory loads at the rotor hub. Therefore, a detailed comparison was made of the $3-10P$ components of the airload. Figure 8 presents a time history of the unsteady airload at r/R = 0.9 in the +5-deg case just discussed. This result was obtained by Fourier decomposing both the measured and predicted loads and removing all the components except those in the specified range. The ability of the present analysis to correlate both the qualitative and quantitative features of the vibratory loading is encouraging. However, a similar calculation run using identical aerodynamic and dynamic models, but with a wake consisting of a single tip filament, produced much less satisfactory results, as is clear from Fig. 8.

The complexity of the actual wake structure in high-speed flight is well illustrated by the top view of the rotor wake geometry given in Fig. 9 for the shaft angle +5-deg case. This figure shows only one "snapshot" of the wake geometry, and

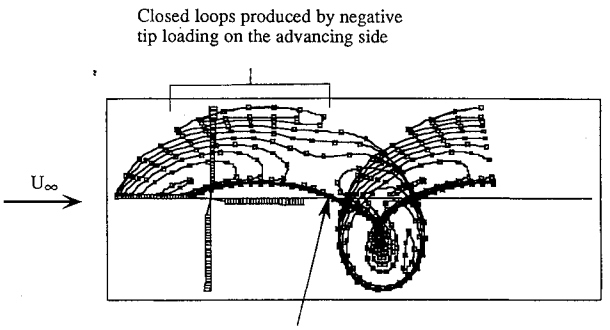

Fig. 9 Top view of the wake of one blade of the H-34 rotor, reference blade at azimuth angle 180 deg. One and one-quarter turns of full-span free wake shown.

for clarity only the wake of one blade is shown. In addition, only the wake in the immediate vicinity of the rotor disk is included. The major features of the wake-induced velocity that contribute to the vibratory loading shown in Fig. 8 can be inferred from this figure. The "down – up" pulse in airload evident in the vicinity of $\psi = 0$ deg is attributable in part to the close approach of the rotor blade to the rolled-up wake trailed from the inboard part of the blade, a phenomenon absent from the simplified wake models using a single-tip vortex. Also, the encounter of the blade with the distributed vorticity in the first and second quadrants as well as with the opposite-sign vorticity trailing from the negatively loaded tip region plays a significant role in determining the crucial up – down event in the first and second quadrants. Again, a single-filament model would fail to capture even the qualitative aspects of the loading generated by a wake with this type of structure.

VII. Summary

The primary objective of this article has been to describe the implementation of a comprehensive analysis of rotorcraft aerodynamics that utilizes a full-span, CVC, free-wake model. The formulation and implementation of the CVC free-wake model was described in some detail. The major features of the vortex lattice aerodynamic model of the blade and the finite element structural model of the blade have been outlined. Correlation results were presented for configurations where wake/blade interaction is of particular importance in modeling aerodynamic loads. Though the focus of the correlation studies presented was high-speed cases, the CVC approach is applicable to simulations of the rotor wake of helicopters and tiltrotors in both high- and low-speed flight. Good correlation was achieved with the H-34 flight test data, with some exceptions at particular radial stations. Comparisons with high-speed runs using the H-34 wind-tunnel data set also produced generally favorable results both for overall loading at inboard stations and for stations near the rotor tip. A discussion of the relation of higher harmonic loading to wake structure showed that significant features of the vibratory airloading of the H-34 absent from predictions made with simplified wake models were captured using the full-span CVC wake. This confirms that the use of an adequately refined wake model is an essential prerequisite for accurate prediction of vibratory airloads in forward flight.

Acknowledgments

This work was sponsored by the Rotorcraft Aeromechanics Branch of NASA Ames Research Center under Contract NAS2-12838. The Technical Monitors were T. L. Norman and R. M. Heffernan.

References

[1]Miller, R. H., "Rotor Blade Harmonic Air Loading," *AIAA Journal*, Vol. 2, No. 7, 1964, pp. 1254 – 1269.

[2]Scully, M. P., "Computation of Helicopter Rotor Wake Geometry and Its Influence on Rotor Harmonic Airloads," Massachusetts Inst. of Technology Aeroelastic and Structures Research Lab., ASRL TR 178-1, Cambridge, MA, March 1975.

[3]Egolf, T. A., and Landgrebe, A. J., "Helicopter Rotor Wake Geometry and Its Influence in Forward Flight," Vol. I, NASA CR 3726, Oct. 1983.

[4]Sadler, S. G., "Main Rotor Free Wake Geometry Effects on Blade Air Loads and Response for Helicopters in Steady Maneuvers," NASA CR 2110 and 2111, Sept. 1972.

[5]Johnson, W. J., "A Comprehensive Analytical Model of Rotorcraft Aerodynamics and Dynamics," NASA TM 81182, June 1980.

[6]Hooper, W. E., "The Vibratory Airloading of Helicopter Rotors," *Vertica*, Vol. 8, No. 2, 1984, pp. 1 – 15.

[7]Miller, R. H., and Ellis, S. C., "Prediction of Blade Airloads in Hovering and Forward Flight Using Free Wakes," *Proceedings of the European Rotorcraft Forum*, Paper 19, 1986.

[8]Johnson, W. R., "Wake Model for Helicopter Rotors in High Speed Flight," NASA CR 177507, Nov. 1988.

[9]Egolf, T. A., "Helicopter Free Wake Prediction of Complex Wake Structures Under Blade-Vortex Interaction Conditions," *Proceedings of the 44th Annual Forum of the American Helicopter Society*, American Helicopter Society, Alexandria, VA, 1988, pp. 819 – 832.

[10]Bliss, D. B., Dadone, L. U., and Wachspress, D. A., "Rotor Wake Modeling for High Speed Applications," *Proceedings of the 43rd Annual Forum of the American Helicopter Society*, American Helicopter Society, Alexandria, VA, 1987, pp. 17 – 33.

[11]Quackenbush, T. R., Bliss, D. B., Wachspress, D. A., and McKillip, R. M., "Free Wake Analysis of Rotor Configurations for Reduced Vibratory Airloads," *Proceedings of the AHS National Specialists' Meeting* (Arlington, TX), American Helicopter Society, Alexandria, VA, 1989.

[12]Quackenbush, T. R., Bliss, D. B., and Wachspress, D. A., "Preliminary Development of an Advanced Free Wake Analysis of Rotor Unsteady Airloads," Continuum Dynamics, Inc. NASA Ames Final Rept., Contract NAS2-12554, Aug. 1987.

[13]Quackenbush, T. R., Bliss, D. B., Wachspress, D. A., Boschitsch A. H., and Chua, K., "Computation of Rotor Aerodynamic Loads in Forward Flight Using a Full-Span Free Wake Analysis," NASA CR 177611, Oct. 1990.

[14]Boschitsch, A. H., and Quackenbush, T. R., "Prediction of Rotor Aeroelastic Response Using a New Coupling Scheme," AIAA Paper 94-2269, June 1994.

[15]Bridgeman, J. O., Strawn, R. C., Caradonna, F. X., and Chen, C. S., "Advanced Rotor Computations with a Corrected Potential Method," *Proceedings of the 48th Annual Forum of the American Helicopter Society*, American Helicopter Society, Alexandria, VA, 1989, pp. 563 – 578.

[16]Strawn, R. C., and Barth, T. J., "A Finite-Volume Euler Solver for Computing Rotary-Wing Aerodynamics on Unstructured Meshes," *Journal of the American Helicopter Society*, Vol. 38, No. 2, 1993, pp. 61 – 67.

[17]Wake, B. E., and Sankar, L. N., "Solutions of the Navier-Stokes Equations for the Flow About a Rotor Blade," *Journal of the American Helicopter Society*, Vol. 34, No. 2, 1989, pp. 13 – 23.

[18]Torok, M., and Berezin, C., "Aerodynamic and Wake Methodology Evaluation Using Model UH-60A Experimental Data," *Journal of the American Helicopter Society*, Vol. 39, No. 2, 1994, pp. 21 – 29.

[19]Quackenbush, T. R., Bliss, D. B., Wachspress, D. A., and Boschitsch, A. H., "Analysis of Rotor Vibratory Loads Using Higher Harmonic Pitch Control," NASA CR 189591, April 1992.

[20]Quackenbush, T. R., Wachspress, D. A., and Boschitsch, A. H., "Computation of Rotor Aerodynamic Loads with a Constant Vorticity Contour Free Wake Model," AIAA Paper 91-3229, Sept. 1991.

[21]Quackenbush, T. R., Lam, G. C.-M., Wachspress, D. A., and Bliss, D. B., "Computational Analysis of High Resolution Unsteady Airloads for Rotor Aeroacoustics," NASA CR 194894; also "Analysis of High Resolution Unsteady Airloads for Helicopter Rotor Blades," *Proceedings of the 50th Annual Forum of the American Helicopter Society*, American Helicopter Society, Alexandria, VA, 1994, pp. 1233 – 1248.

[22]Bliss, D. B., Quackenbush, T. R., and Bilanin, A. J., "A New Methodology for Helicopter Free Wake Analyses," *Proceedings of*

the 39th Annual Forum of the American Helicopter Society, American Helicopter Society, Alexandria, VA, 1983, Paper 83-39-75-0000.

[23]Bliss, D. B., Teske, M. E., and Quackenbush, T. R., "A New Methodology for Free Wake Analysis Using Curved Vortex Elements," NASA CR 3958, Dec. 1987.

[24]Quackenbush, T. R., "Computational Studies in Low Speed Rotor Aerodynamics," *Proceedings of the AHS National Specialists' Meeting on Rotor Aerodynamics and Aeroacoustics*, American Helicopter Society, Alexandria, VA, 1987.

[25]Quackenbush, T. R., Bliss, D. B., Wachspress, D. A., and Ong, C. C., "Free Wake Analysis of Hovering Performance Using a New Influence Coefficient Method," NASA CR 4309, July 1990.

[26]Rubbert, P. E., "Theoretical Characteristics of Arbitrary Wings by a Nonplanar Vortex Lattice Method," The Boeing Co., Rept. 06-9244, May 1964, Seattle, WA.

[27]Margason, R. J., and Lamar, J. E., "Vortex Lattice FORTRAN Program for Estimating Subsonic Aerodynamic Characteristics of Complex Planforms," NASA TN-D 6142, Sept. 1971.

[28]Chiu, Y. D., "Convergence of Discrete-Vortex Induced-Flow Calculations by Optimum Choice of Mesh," Ph.D. Dissertation, Georgia Inst. of Technology, School of Aerospace Engineering, Atlanta, GA, Aug. 1988.

[29]Celi, R., and Friedmann, P. P., "Aeroelastic Modeling of Swept Tip Rotor Blades Using Finite Elements," *Journal of the American Helicopter Society*, Vol. 33, No. 2, 1988, pp. 43–52.

[30]Quackenbush, T. R., Boschitsch, A. H., Wachspress, D. A., and Chua, K., "Rotor Design Optimization Using a Free Wake Analysis," NASA CR 177612, April 1992.

[31]Rabbott, J. P., Jr., Lizak, A. A., and Paglino, V. M., "A Presentation of Measured and Calculated Full-Scale Rotor Blade Aerodynamic and Structural Loads," USAAVLABS, TR 66-31, July 1966.

[32]Scheiman, J., "A Tabulation of Helicopter Rotor-Blade Differential Pressures, Stresses, and Motions Measured in Flight," NASA TM-X 952, March 1974.

[33]Heffernan, R. M., and Gaubert, M., "Structural and Aerodynamic Loads and Performance Measurements of an SA349/2 Helicopter with an Advanced Geometry Rotor," NASA TM-88370, Nov. 1986.